Clinical Plasma Medicine 1 (2013) 36–44

Contents lists available at SciVerse ScienceDirect

Clinical Plasma Medicine

journal homepage: www.elsevier.com/locate/cpme

# *Ex vivo* human skin experiments for the evaluation of safety of new cold atmospheric plasma devices

G. Isbary [a,*,1], J. Köritzer [b,1], A. Mitra [b], Y.-F. Li [b], T. Shimizu [b], J. Schroeder [d], J. Schlegel [c], G.E. Morfill [b], W. Stolz [a], J.L. Zimmermann [b]

[a] Department of Dermatology, Allergology and Environmental Medicine, Hospital Munich Schwabing, Koelner Platz 1, 80804 Munich, Germany
[b] Max Planck Institute for Extraterrestrial Physics, Giessenbachstrasse, 85748 Garching, Germany
[c] Department of Pathology, Technical University of Munich, Trogerstr. 18, 81675 Munich, Germany
[d] Department of Pathology, University of Regensburg, Franz-Josef-Strauss-Allee 11, 93053 Regensburg, Germany

ARTICLE INFO

*Article history:*
Received 6 July 2012
Received in revised form
28 September 2012
Accepted 9 October 2012
Availabla online 12 December 2012

*Keywords:*
Plasma medicine
Cold atmospheric plasma
Plasma
H2AX
Chronic wounds
Clinical trial

ABSTRACT

Cold atmospheric plasma is an innovative tool in medicine and hygiene. However, there are no regulations or recommendations for experiments to prove the safety of upcoming devices yet. Healthy *ex vivo* human skin samples were treated with new upcoming plasma devices (FlatPlaSter 2.0 and MiniFlatPlaSter) for safety purposes. The results indicate—besides the safety measurements/calculations of toxic by-products ($O_3$, NO, and $NO_2$) and the UV power density—that a plasma treatment of up to 2 min is tolerable for the skin (histology and electron microscopy experiments) and safe concerning DNA damages (gamma-H2AX stain assay).

© 2012 Elsevier GmbH. All rights reserved.

## 1. Introduction

Cold atmospheric plasma (CAP) has gained more and more attention in the scientific community, due to its promising antimicrobial features. Already a multitude of publications about the broad antimicrobial spectrum of CAPs have been published—especially on different pathogens, such as various bacteria including multi-resistant strains, biofilms, spores, fungi and even viruses [1–8]. Other publications demonstrated the benefit of a CAP treatment compared with other products in use or an advantage in application due to its physical and chemical properties [9–12]. Furthermore a lot of investigations concerning the safety of CAPs on mammalian cells and tissue have been carried out: these included detailed toxicity and mutagenicity analysis, AFM images of different treated cell lines, investigations of treated human blood, a modified HET-CAM test or the capability to stimulate different cell lines (e.g. fibroblasts) and so on [12–19]. In other words many approaches from different groups all over the world have started to evaluate the efficacy and safety of their respective CAP devices. Last but not least already 7 years of clinical experience of first trials using microwave driven argon CAP devices *in vivo* has been obtained where no side effects or allergic reactions occurred up to now and new clinical trials of several groups in Germany are currently under investigation [20–23].

Nevertheless, up to now there is no agreement within the constantly increasing number of research groups for recommended, useful and also necessary experiments for safety features of CAP devices before targeting on clinical trials. If one considers, that the CAP devices differ enormously in design and in composition of the generated plasma—depending on the used technology and gas to produce the plasma (e.g. Dielectric Barrier Discharge (DBD), Surface Micro Discharge (SMD) technology, microwave driven plasma, plasma pen, plasma bullets, etc.)—it is without doubt necessary to implement at least a small number of experiments that are needed to be performed by each group besides other obligatory tests before implementing a new technical device, which can vary on regional, national, Europe-wide, American or international needs (e.g. tests on electromagnetic compatibility, a test report of medical electrical equipment, a risk assessment, a positive evaluation of an independent notified body, the approval of a competent federal authority, the approval of medical ethics committee and others). These safety tests should include on the one hand safety measurements of toxic by-products generated during plasma production and operation, such as the emitted light especially in the range of UVC and toxic reactive species (e.g. $O_3$, NO, $NO_2$) [21,24–26]. On the other hand

*Abbreviations:* AFM, Atomic Force Microscopy; CAP, Cold Atmospheric Plasma; DBD, Dielectric Barrier Discharge; SMD, Surface Micro-Discharge; UV, Ultraviolet

* Corresponding author. Tel.: +49 89 3068 2904; fax: +49 89 3068 7522.
*E-mail address:* dr.isbary@googlemail.com (G. Isbary).

[1] Both authors contributed equally.

2212-8166/$ - see front matter © 2012 Elsevier GmbH. All rights reserved.
http://dx.doi.org/10.1016/j.cpme.2012.10.001

the evaluation of mutagenicity, toxicity and skin tolerability must be demonstrated.

In this paper we want to demonstrate 3 easy to realize experiments of *ex vivo* treated healthy human skin samples. The first test is based on a histological evaluation, the second investigates the samples on the basis of electron microscopy (EM) and the last test uses γ-H2AX staining to detect double strand breaks in DNA. We want to suggest these experiments as a possible safety standard for upcoming plasma devices where an application on human skin is targeted.

## 2. Materials and methods

### 2.1. Sample selection criteria

Patients (all Caucasians) who attended the inpatient Clinics of the Department of Dermatology, Allergology and Environmental Medicine of Hospital Munich-Schwabing, Germany were invited to provide skin samples for research purposes. All patients gave their oral and written informed consent prior to the excisions and the experiments were performed according to the Declaration of Helsinki principles. Table 1 summarizes the patients' characteristics. These skin samples were collected during necessary tumor excisions. The used skin samples obtained for skin tests were collected from lateral triangles of skin spindles (necessary for tension-free cosmetic closures) outside of the safety margins of tumor excisions. Total excision area was not larger than needed for cosmetic closure for all patients.

The clinical trial did not need approval by the ethics committee of the Bavarian State Association for Medical Issues according to §15, however the ethics committee was informed about procedure. The committee determined that the procedure is in accordance to §15.

### 2.2. Used CAP devices

Both CAP devices (FlatPlaSter 2.0 and MiniFlatPlaSter) used in this study possess electrodes based on the Surface Micro Discharge (SMD) technology, which has been published in detail in Morfill et al. [4]. The characterization of the devices is in the results section.

#### 2.2.1. Experimental setup for the FlatPlaSter 2.0

The plasma electrode of the FlatPlaSter 2.0 (Fig. 1) has a size of $13 \times 9$ cm$^2$ and consists of a Teflon plate, which is sandwiched by a brass planar plate and a stainless steel mesh grid. By applying a sinusoidal voltage of 8.5 kV$_{pp}$ with a frequency of 1 kHz, microdischarges are produced in the surrounding air on the mesh grid of the electrode. The power consumption for the plasma discharge is approximately 0.02 W/cm$^2$ and was measured with the Lissajous method using a 1 μF capacitance [27].

**Table 1**
Summary of the patients' characteristics.

| Number | Gender | Age | Disease | Localization |
|---|---|---|---|---|
| 1 | Female | 93 | Bowen's disease/carcinoma | Back |
| 2 | Male | 52 | Melanoma | Upper arm |
| 3 | Male | 84 | Basal cell carcinoma | Lower leg |
| 4 | Male | 44 | Melanoma (SSM) | Chest |
| 5 | Male | 71 | Melanoma (SSM) | Upper arm |
| 6 | Female | 71 | Melanoma (nodular) | Back |
| 7 | Female | 68 | Melanoma (nodular) | Forearm |
| 8 | Male | 67 | Melanoma (SSM) | Back |

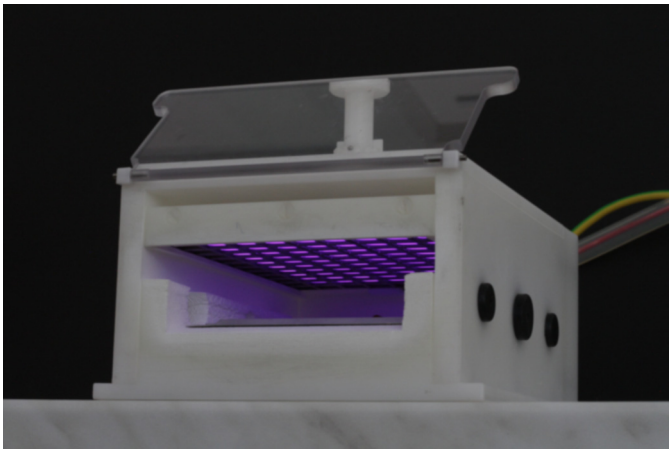

**Fig. 1.** FlatPlaSter 2.0 which incorporates a SMD electrode inside. During the plasma treatment of human skin samples—which are placed beneath the electrode—the door of the device is closed to confine the species, produced by the plasma, inside. The transport of plasma species to the skin samples is diffusive—no ventilator etc. was used.

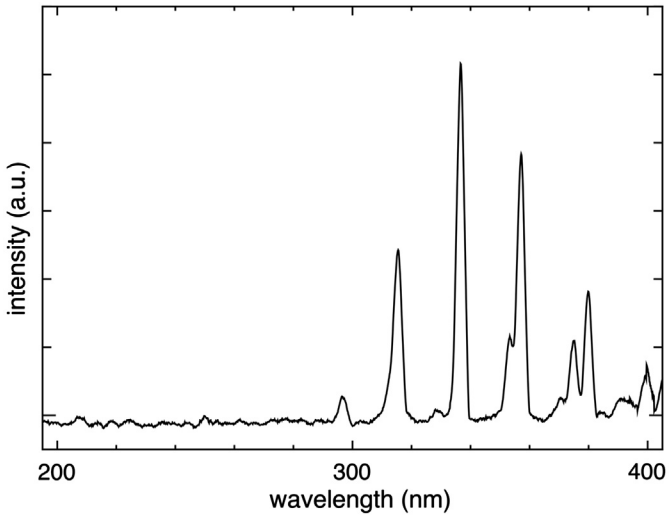


**Fig. 2.** Emission spectrum of the FlatPlaSter 2.0 in the range of 200–400 nm.

The plasma electrode itself is incorporated in a POM-C box and located at the top. During the plasma treatment the door of the POM-C box can be closed to confine the species produced by the plasma inside.

#### 2.2.2. Experimental setup for the MiniFlatPlaSter

The electrode of the MiniFlatPlaSter (Fig. 3a) has a diameter of 2.8 cm and is based on the same SMD technology used in the FlatPlaSter 2.0. Designed for portable usage the MiniFlatPlaSter incorporates the high voltage power supply for plasma generation inside. The round shaped electrode—located at the top of the device—consists of a glass Epoxy board, which is sandwiched by a copper foil layer and a stainless steel mesh grid. As mentioned above the plasma is produced in the ambient air on the side of the mesh grid by applying a high pulse-like voltage of 7 kV$_{pp}$ with a repetition frequency of 6.75 kHz. The used voltage waveform is presented and explained in Maisch et al. [2]. The power consumption is approximately 0.5 W/cm$^2$.

The human skin samples were treated—in this case—under "open conditions" with a distance of approximately 2–3 mm between the electrode and the stainless steel mesh grid (Fig. 3b).

### 2.3. Treatment protocol

Treatment modalities are summarized in Table 4.

#### 2.3.1. Assessment of safety in histology experiments

Histology experiments were carried out with the FlatPlaSter 2.0 and the MiniFlatPlaSter. All skin samples were collected directly after excision from operating suite and placed into a petri dish containing 0.9% $NaCl_2$ to prevent desiccation. The skin surface was not covered with 0.9% $NaCl_2$. Using a scalpel the collected skin samples were cut into slices larger than a 5 mm punch biopsy.

The following CAP treatment procedure was carried out with the FlatPlaSter 2.0.

The petri dish including the human skin sample(s) was placed in the middle of the FlatPlaSter 2.0 device. The distance between the SMD electrode and the skin surface was approximately 6–7 mm. During the CAP treatment the door of the device was closed. During the breaks the lid of the device was opened to filter the volume and afterwards to exchange the air in between the different treatments.

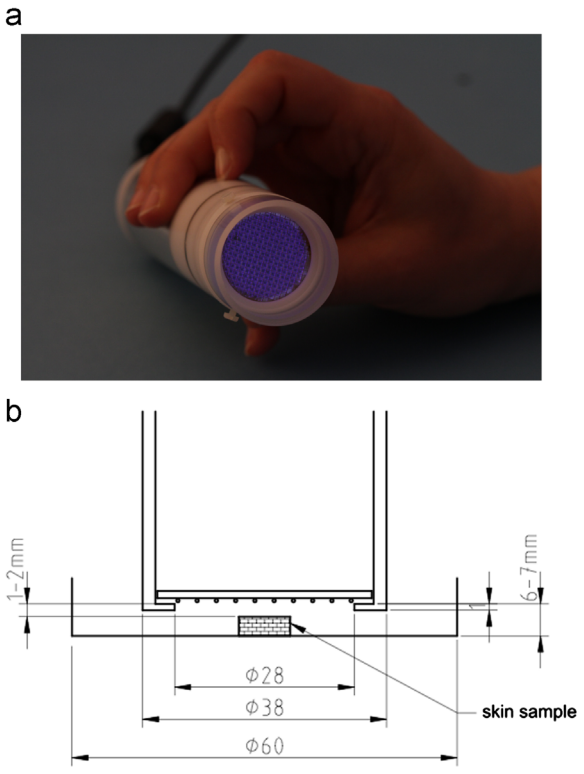


**Fig. 3.** (a) MiniFlatPlaSter for portable usage. The round shaped SMD electrode has a diameter of 2.8 cm. The species produced by the plasma are transported via diffusion to the samples to treat. (b) Sketch of the experimental setup for treatment of human skin samples in an "open volume".

The following treatment procedure was carried out with the MiniFlatPlaSter.

The petri dish including the human skin sample(s) was placed directly beneath the SMD electrode of the MiniFlatPlaSter. The distance between the electrode and the skin surface was approximately 2–3 mm and the CAP exposure was carried out under "open conditions". The device was not used in the accumulator driven mode but in the power adaptor mode.

Controls were kept under equal conditions just as the samples treated with the FlatPlaSter 2.0 and the MiniFlatPlaSter device, including the additional drop of 0.9% $NaCl_2$ on top of the samples during breaks, or not.

After the final plasma treatment or control time using either the FlatPlaSter 2.0 or the MiniFlatPlaSter device, the samples were fixed in 4% of formalin for further processing. Fixation processes were realized using a certified automated Shandon Excelsior A78410110 device (ThermoFisher Scientific, Waltham, MA, United States). After cooling down the probes to $-3$ to $-4$ °C, samples were cut into 3 µm slices using a Micron HM340E device (ThermoFisher Scientific, Waltham, MA, United States). Hematoxylin and eosin staining was realized using automated Tissue Stainer TST44C Medite GmbH, Burgdorf, Germany.

#### 2.3.2. Assessment of safety in electron microscopy experiments

For EM experiments only samples of patient 2 and 3 (treated with the FlatPlaSter 2.0) were investigated due to the highest CAP treatment time. Both samples had identical treatment modalities as for the histology experiments, were fixed in 0.1 M cacodylate-buffered Karnovsky solution (2.5% glutaraldehyde and 1% paraformaldehyde; overnight, room temperature) and sent to the Department of Pathology, University of Regensburg, Germany, the next day.

Small tissue samples (approx. 1 $mm^3$) were routinely postfixed in 1% osmium tetroxide (2 h) at pH 7.3; dehydrated in graded ethanols, and embedded in the EmBed-812 epoxy resin (all reagents from Science Services, Munich, Germany). After 48 h heat polymerisation at 60 °C, semithin (0.8 µm) sections were cut, stained with toluidine blue/basic fuchsin, and after selection of appropriate areas of interest the Epon block was trimmed for ultrathin sectioning. Ultrathin (80 nm) sections were cut with a

**Table 3**
Dispersed concentrations of reactive species (during the CAP treatment using the MiniFlatPlaSter) compared with the NIOSH safety limits for 8 h continuous inhaling [29].

| Reactive species (RS) | Volume concentrations $\langle c_i \rangle$ | Dispersed concentrations ($c_{Rsi}$) | Safe values (NIOSH) |
|---|---|---|---|
| $O_3$ | 25 ppm | $1.16 \times 10^{-4}$ ppm | 0.1 ppm |
| NO | $<1$ ppm | $4.64 \times 10^{-6}$ ppm | 25 ppm |
| $NO_2$ | $<35$ ppm | $1.63 \times 10^{-4}$ ppm | 5 ppm |

**Table 2**
Characteristics of the MiniFlatPlaSter.

| | | |
|---|---|---|
| Charged particles | Electrons, ions | $\sim 10^{11}$ $cm^3$ |
| Reactive species | $O_3$ | Mean value for a treatment time of 2 min ~25 ppm |
| | NO | Mean value for a treatment time of 2 min $<1$ ppm |
| | $NO_2$ | Mean value for a treatment time of 2 min $<35$ ppm |
| Heat | | At maximum 8° increase (referring to the ambient temperature) |
| Photons | UV, visible | Power density $<0.6$ µW/$cm^2$ |
| Static electric field | | $\sim 10^7$ V/m on the mesh electrode |
| Electrical current through the samples | | $<50$ nA/$cm^2$ |

**Table 4**
Summary of the treatment modalities.

| Pat. nr. | Sample | Experiment | Device | Total treatment time | Mode | Break | 0.9% NaCl drops on sample/control |
|---|---|---|---|---|---|---|---|
| 1 | 1 | Histology | FlatPlaSter 2.0 | 300 s | Continous | No | No |
| | 2 | Histology | FlatPlaSter 2.0 | 2 × 300 s | Continous | 60 s | 1 × after 300 s |
| 2 | 1 | Histology/electron microscopy | FlatPlaSter 2.0 | 4 × 300 s | Continous | 3 × 60 s | 1 × after each 300 s |
| 3 | 1 | Histology/electron microscopy | FlatPlaSter 2.0 | 4 × 300 s | Continous | 3 × 60 s | 1 × after each 300 s |
| 4 | 1 | Histology | MiniFlatPlaSter | 2 × 120 s + 60 s | Continous | 2 × 30 s | No |
| | 2 | Histology | MiniFlatPlaSter | 5 × 120 s | Continous | 4 × 30 s | 1 × after 360 s |
| 5 | 1 | Histology | MiniFlatPlaSter | 10 × 120 s | Continous | 9 × 30 s | 1 × after 360 s and 720 s |
| | 2 | Histology | MiniFlatPlaSter | 10 × 120 s | Continous | 9 × 30 s | 1 × after each 120 s |
| 6 | 1 | Gamma H2AX | MiniFlatPlaSter | 30 s | Continous | No | No |
| | 2 | Gamma H2AX | MiniFlatPlaSter | 60 s | Continous | 30 s | 1 × after 30 s |
| | 3 | Gamma H2AX | MiniFlatPlaSter | 240 s | Continous | 3 × 30 s | 1 × after 30 s, 60 s, 120 s |
| | 4 | Gamma H2AX | MiniFlatPlaSter | 360 s | Continous | 4 × 30 s | 1 × after 30 s, 60 s, 120 s, 240 s |
| | 5 | Gamma H2AX | MiniFlatPlaSter | 480 s | Continous | 5 × 30 s | 1 × after 30 s, 60 s, 120 s, 240 s, 360 s |
| 7 | 1 | Gamma H2AX | MiniFlatPlaSter | 60 s | Continous | No | No |
| | 2 | Gamma H2AX | MiniFlatPlaSter | 120 s | Continous | 30 s | 1 × after 60 s |
| 8 | 1 | Gamma H2AX | MiniFlatPlaSter | 30 s | Continous | No | No |
| | 2 | Gamma H2AX | MiniFlatPlaSter | 60 s | Continous | 30 s | 1 × after 30 s |
| | 3 | Gamma H2AX | MiniFlatPlaSter | 120 s | Continous | 2 × 30 s | 1 × after 30 s, 60 s |

diamond knife on a Reichert Ultracut-S ultramicrotome and double contrasted with aqueous 2% uranyl acetate and lead citrate solutions for 10 min each. The sections were examined in a LEO912AB electron microscope operating at 80 kV (Oberkochen, Germany; digital imaging = 1 k × 1 k pixel side-entry CCD-Camera, TRS, Morenweiss, Germany, iTEM-Software, OSIS, Muenster, Germany).

### 2.3.3. Assessment of safety using H2AX staining

CAP treatment was carried out *ex vivo* with the MiniFlatPlaSter. The distance between the skin sample and the electrode was 2–3 mm. Skin samples were placed in petri dishes and were kept in 0.9% $NaCl_2$ to prevent desiccation until the CAP treatment was achieved. Treatment times varied between 30 s and 8 min. Punch biopsies (size 5 mm) were taken after the CAP treatment and the remaining tissue was further CAP treated. Controls were handled equally. 0.9% $NaCl_2$ was exchanged after each treatment to prevent changes due to the plasma treatment.

Directly after the CAP treatment, skin samples were put in 4% formaldehyde for at least 24 h followed by an embedment in paraffin. Paraffin embedded tissue was cut in 2 μm sections and mounted on glass slides for incubation at 50 °C.

For immunohistochemistry the Dako REAL™ Detection System Peroxidase/DAB + Kit (K 5001) (Dako, Jena, Germany) was used according to the protocol with slight modifications. Briefly, slices were de-paraffinized and then thoroughly washed in 1 × phosphate buffered saline (PBS). For heat-mediated antigen retrieval, slides were placed in 1 × sodium citrate buffer, pH 6.0 heated to 95 °C. Total heating time in the citrate buffer in the steamer was 7 min. Slides were allowed to cool down for 30 min at room temperature. Slides were washed three times in 1 × PBS for a total of 15 min and then incubated for further 15 min in 3% $H_2O_2$ at room temperature. After three additional washing steps, samples were blocked with Avidin/Biotin for 15 min. Pre-incubation with 5% normal goat serum for 30 min at room temperature occurred before and the slices were then incubated overnight at 4 °C with the following primary antibody rabbit polyclonal anti-gamma H2A.X (1:300; Cell Signaling Technology Inc., Danvers, MA, United States) in 1 × PBS containing 5% normal goat serum. The following day, each slide was washed in 1 × PBS and incubated in secondary antibodies (antibody A and complex B) for 30 min at 37 °C. Slides were washed in 1 × PBS and DAB (concentrations according to the Dako protocol) and mounted onto the slides for 5–10 min. Afterwards, the slides were washed with tap water followed by nuclei staining with haemalm. Slides were then covered with glass coverslips.

## 2.4. Analysis of the results

Histological evaluation of the samples was performed in a blinded way by histopathologists of the Department of Dermatology, Allergology and Environmental Medicine of Hospital Munich—Schwabing, Germany.

Evaluation of EM images were realized in a blinded way by the Department of Pathology, University of Regensburg, Germany

Microscopy and image processing of H2AX stained slides: The images were acquired with a Hamamatsu Nanozoomer 2.0 HT using a 40 × magnification. The light intensity, image resolution and the signal settings were kept constant for all the set of slides used in this experiment. The scale was kept constant throughout the experiments.

The images were exported separately as tiff files and processed using the Image J software (U.S. National Institute of Health, http://rsbweb.nih.gov/ij/) with customized macros. The series of images were imported using "File\import\image sequence" and processed with "substract background (keeping rolling ball radius 10 pixel)" and "brightness/contrast adjustment". The threshold value for γ-H2AX was adjusted manually using "Threshold colour plugin" in RGB mode until visually best fits were observed between the original and the processed images. To differentiate between normal and γ-H2AX stained cells, we processed the slides in RGB format and then counted them in 8 bit format using "Analyze/Analyze particles".

## 2.5. Data analysis

Data was entered, checked and analyzed using IDL 7.0 (ITT Visual Information Solutions, Boulder, Colorado, United States). Results in *y*-axis give the mean ratio of stained (brown) cells (i.e. cells possessing DNA double strand breaks)/total number of cells including standard deviation. For statistical evaluation Wilcoxon test was applied, *p*-values of 0.01–0.05 were considered as significant, $p < 0.01$ as highly significant.

## 3. Results

### 3.1. Patient characteristics

Included eight patients (three females, average age 68.6 years, ranged from 44 to 93 years) which suffered from different skin tumors (melanoma—nodular or superficial spreading, basal cell carcinoma or advanced Bowen's disease). Table 1 summarizes the patients' characteristics.

### 3.2. Characterization of the devices

#### 3.2.1. Characterization of the FlatPlaSter 2.0

The main constituents produced by the FlatPlaSter 2.0 have been measured and summarized in Maisch et al. [2]. In short, for the treatment times used in this study, the temperature increased to at maximum 4° above the ambient temperature. The main UV components of the emission spectrum (Fig. 2) are in the wavelength range between 280 and 400 nm. Furthermore, lines in the UVC region of the spectrum can be detected. The UV power density was measured to be 25 nW/cm$^2$. This value is even for longer plasma treatment times of up to 20 min far below the ICNIRP (International Commission Non-Ionizing Radiation Protection) safety level for intact human skin (maximum UV dose by ICNIRP for healthy intact skin is 3 mJ/cm$^2$) [28].

Concerning the toxic gas production of the FlatPlaSter 2.0 mean values of the concentrations, $c$, of approximately 500 ppm for $O_3$, $< 1$ ppm for NO and 3 ppm for $NO_2$ were measured at the end of the application. The measurement of $O_3$ (using optical emission spectrometry) was carried out under closed conditions (i.e. the door of the FlatPlaSter 2.0 box was closed). The measured $O_3$ value inside the box is above the NIOSH (National Institute for Occupational Safety and Health) limit of 0.1 ppm for 8 h continuous inhaling for all used treatment times [29]. The $O_3$ value likely to be inhaled by the user, if all produced $O_3$ escapes and disperses in the room is calculated as follows.

If the FlatPlaSter 2.0 box is opened after the CAP treatment, an application volume $V_a$ of $13 \times 9 \times 0.7$ cm$^3$ = 81.9 cm$^3$ (size of the electrode $13 \times 9$ cm$^2$; height to the skin sample 6–7 mm) containing $O_3$ is allowed to disperse in the room. Assuming no losses of $O_3$ by decomposition, recombination, surface adsorption etc. we can calculate the maximum concentration of $O_3$ after dispersal in 1 m$^3$ of air. This is taken to be the usual distance for inhalation purposes.

The $O_3$ concentration is then $c_{Air}$, where $c_{Air} \equiv c_i(t) \times 10^{-6} 1/(\mathrm{cm}^3) V_a$ with $c_i(t)$ the measured value inside the closed volume.

According to NIOSH the maximum safe value for $c_{Air}$ is $< 0.01$ ppm for 8 h continuous inhaling [29]. (Note that in our case, inhalation time is of order minutes—before ozone is removed by natural processes).

The NIOSH limit implies, that the measured $O_3$ value inside the FlatPlaSter 2.0 device has to be $c_i(t) \leq 0.1\ \mathrm{ppm} \times (10^6 \mathrm{cm}^3/V_a) = 1221$ ppm. Our measured value of 500 ppm is below this (even for 8 h inhalation). Nevertheless—for safety purposes—the volume inside the FlatPlaSter 2.0 box was filtered after each CAP treatment using a carbon filter.

The NO and $NO_2$ values were measured under open conditions (i.e. the door of the FlatPlaSter 2.0 box was open). These values ($< 1$ ppm (NO) and 3 ppm ($NO_2$)) are far below the safety limits provided by NIOSH (25 ppm (NO) and 5 ppm ($NO_2$)) for 8 h constant exposure/inhaling even without taking into account the dispersion in air [29].

As the FlatPlaSter 2.0 produces the plasma indirectly—i.e. the treated sample does not function as the counter electrode—the electrical current through the human skin sample is negligible (below 100 μA) [30].

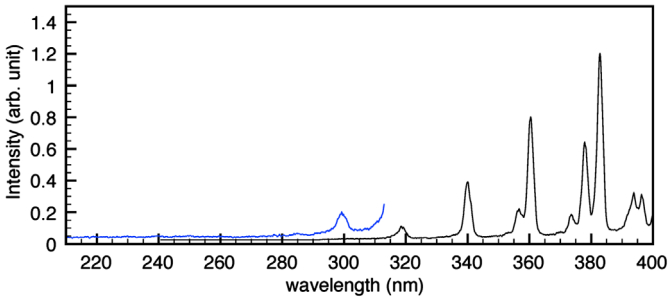


**Fig. 4.** Emission spectrum of the MiniFlatPlaSter in the range of 200–400 nm. The blue line in the shorter wavelength range is scaled up in order to highlight the peak around 300 nm. (For interpretation of the references to color in this figure legend, the reader is referred to the web version of this article).

#### 3.2.2. Characterization of the MiniFlatPlaSter

The main constituents produced by the MiniFlatPlaSter are listed in Table 2.

Fig. 4 shows the emission spectrum of the MiniFlatPlaSter where the main UV components are in the wavelength range between 280 and 400 nm. The UV power density was measured to be less than 0.6 μW/cm$^2$. For a plasma treatment time of 10 s the UV dose of the MiniFlatPlaSter therefore is less than 6 μJ/cm$^2$, which is more than a factor 500 below the ICNIRP safety limits [28].

Concerning the toxic gas production of the MiniFlatPlaSter, mean values of 25 ppm for $O_3$, $< 1$ ppm for NO and $< 35$ ppm for $NO_2$ for a treatment time of 2 min were measured close to the plasma electrode.

To estimate the amount of toxic gases inhaled during operation of the device under "open conditions", a calculation—taking into account the diffusive flux leaving the plasma production volume through the gap (between the electrode and the skin surface) during operation and further dispersion in 1 m$^3$ air—was carried out (see below). From these calculations values of $1.16 \times 10^{-4}$ ppm for $O_3$, $4.64 \times 10^{-6}$ ppm for NO and $1.63 \times 10^{-4}$ ppm for $NO_2$ were obtained and can therefore be inhaled during a 2 min plasma treatment. These dispersed values arefar below the safety limits of NIOSH (see Table 3) [29]

Similar to the FlatPlaSter 2.0 the MiniFlatPlaSter also produces the plasma indirectly—without using the skin as a counter electrode. The current through the sample was estimated to be $< 50$ nA/cm$^2$, which even for larger treatment areas of up to 30 cm$^2$ is still far below the safety limits published by ICNIRP and below the value of 100 μA given by the International Standard IEC 60601-1 [28,30].

*3.2.2.1. Calculation of dispersed concentrations of reactive species (MiniFlatPlaSter).* In the "open volume" application of the MiniFlatPlaSter the geometry is cylindrical and given in Fig. 3b. The distance between the electrode and the human skin sample is ~3 mm, the "gap" is $h = 5$ mm, and the radius of the electrode is $R = 1.4$ cm. The transport of reactive species (RS) is assumed to be diffusive. The governing equation (in cylindrical symmetry) for the concentration of species $i$, $c_i = n_{RSi}/n_{Air}$, is

$$\frac{\partial c_i}{\partial t} - \frac{1}{r}\frac{\partial_i}{\partial r} r\kappa \frac{\partial c_i}{\partial r} = \text{source} - \text{losses} \quad (1)$$

where the source is the plasma production rate of species $i$ and losses are due to chemical reactions with other species and absorption on the skin and walls. Considering only diffusion in a

quasi-steady state, we get for the diffusive flux leaving the plasma production volume through the gap

$$F_{Diff} = 2\pi \times Rh\kappa \frac{\partial c_i}{\partial r} n_{Air} \text{ reactive molecules/second} \quad (2)$$

We may simplify this without too much error by noting that the only relevant length scale in the problem is the radius $R$. Then we get

$$F_{Diff} \approx 2\pi \times h\kappa \times c_i n_{Air} \quad (3)$$

The diffusion coefficient $\kappa = 1\lambda\nu/3$, where $\lambda = 1/n_{Air}\sigma_i$ is the mean free path and $\nu$ is the thermal velocity of the RS. $\sigma_i$ is the air–RS collision cross section. Then we get

$$F_{Diff} = \frac{2\pi}{3\sigma_i} h c_i \mathrm{v} \quad (4)$$

The concentration of RS species, $c_i$, varies with time. Hence the total number of RS molecules that escape through the gap is given by

$$N_{RS} = \int_0^t F_{Diff} dt = \frac{2\pi \times h\nu}{3\sigma_i} \int c_i dt \equiv \frac{2\pi \times h\nu \langle c_i \rangle}{3\sigma_i} t \quad (5)$$

$c_i(t)$ is measured, so that we can evaluate expression (5). For typical measured values we take $\langle c_{O_3} \rangle = 25$ ppm, $\langle c_{NO} \rangle = 1$ ppm, $\langle c_{NO_2} \rangle = 35$ ppm (from Table 2).

Furthermore, we again consider dispersal of the escaped RS over 1 $m^3$ before inhalation. For a plasma application time of $t = 120$ s using the typical values $\sigma_i = 10^{-14}$ $cm^2$ and $\nu = 10^4$ cm/s this gives

$$N_{RS} = 1.25 \times 10^{20} \langle c_i \rangle \text{ escaped RS molecules} \quad (6)$$

and a concentration after dispersal in 1 $m^3$ air

$$c_{RSi} = 4.64 \times 10^{-6} \langle c_i \rangle \quad (7)$$

By inserting the measured values (from Table 2) in Eq. (7) we see that the dispersed RS (assuming no losses by dissociation, recombination, adsorption, etc.) is far below the safe inhalation limits (given by NIOSH) for all three species $O_3$, NO and $NO_2$ (Table 3) [29].

The "rest RS" trapped in the volume and released after application would, in the dispersed state (over 1 $m^3$), amount to a $5.52 \times 10^{-7}$ dilution, roughly 12% of the amount that escapes by diffusion (see expression (7)).

Regarding the validity of the diffusion and steady state assumptions, there are two conditions. First the diffusion mean free path $\lambda = 1/n_{Air}\sigma_i$ has to be much smaller than the vertical height $h$. Since $\lambda = 4.4 \times 10^{-6}$ cm this is satisfied. Second, the time scale for diffusion across the gap ($h^2/4\kappa$) has to be smaller than the application time. Substituting values gives a diffusion time scale of 17 s. This is significantly smaller than the application time of 120 s, so that transient effects are likely to be small. However, these would always tend to lower the escape of RS and hence the dispersed concentrations, so that our basic conclusions are not affected.

### 3.3. Outcomes

#### 3.3.1. Histology

No plasma induced changes were found for up to 20 min treated histological specimen compared to the controls (Fig. 5). Changes like actinic elastosis, vacuole degeneration and focal perivascular inflammation occurred in some samples, but in corresponding controls as well.

#### 3.3.2. Electron microscopy

No changes occurred in epidermal and dermal layers of $4 \times 300$ s plasma treated samples compared to the controls (Fig. 6). One sample presented an enlargement of the basement membrane, but in control sample in equal measure.

#### 3.3.3. γ-H2AX

Results of the γ-H2AX staining (Fig. 7) revealed that there are significant higher (patient 6, 4 min, $p \leq 0.05$ and patient 8, 1 min, $p \leq 0.05$), but also significant lower changes (patient 6, 1 min, $p \leq 0.001$ and patient 8, 2 min, $p \leq 0.05$) in detected DNA damages in plasma treated skin samples compared to the controls. However, there was a trend towards higher damages in patients treated with plasma for more than 120 s. Furthermore, the data showed that plasma treatments up to 60 s could be considered as a safe application time using MiniFlatPlaSter. Interestingly, there we found a negative correlation (data not shown) between total cell numbers and cell damages. This means, the higher the initial cell load the less damages were detected. All patients (age range 67–71 years) showed relatively high staining to γ-H2AX.

## 4. Discussion

Expectations towards the CAP technology are high. Therefore the "plasma medicine community" has a great responsibility to set up safety experiments in vitro and *ex vivo* to demonstrate the safety of each device prior to applications *in vivo*. Especially tests are needed which are comprehensive, reproducible and more or less easy to realize for all groups, but also feasible for the broad spectrum of varying plasma devices.

*Ex vivo* experiments with healthy human skin meet these criteria. In all surgical active dermatologic clinics (but also in other medical societies) many operations are carried out where

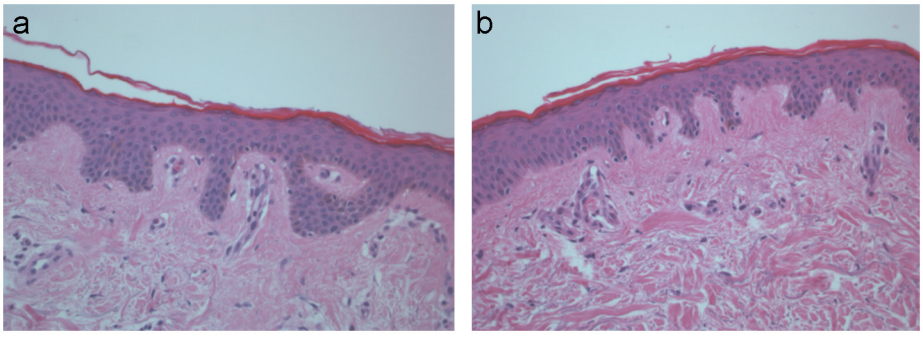


**Fig. 5.** (a) No plasma induced damages of epidermal and dermal layers after $4 \times 300$ s of plasma exposure (FlatPlaSter 2.0) in histology specimen (200× magnification) compared to the control sample (b) were detectable.

excess skin arises due to the operation techniques for cosmetically satisfying closures. Normally excess skin is disposed. The advantage of using *ex vivo* human skin—at least in Germany—is that there is no need for approval of the medical ethics committee according to §15 of the Medical Association's professional code if there is no way to track the patients data back. Histologic samples were therefore stored in anonymous way that only the tutor of the trial can re-track the samples if necessary. The ethics committee was informed about the procedure of the *ex vivo* experiments and stated that everything is in accordance to §15. It is obvious that patients need to sign an informed consent form. The samples should derive from healthy skin and should be large enough to include a control area as well, which is generally the case beyond the safety margins in tumor excisions. *Ex vivo* skin also has the closest transferability to *in vivo* conditions in humans, even with a lack of possible systemic reactions.

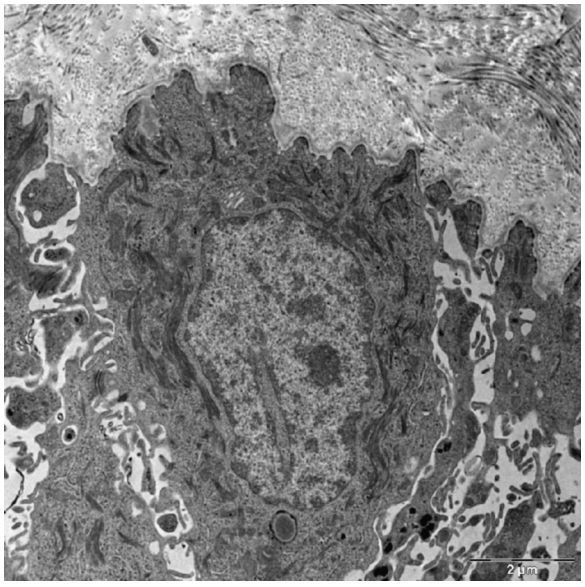

**Fig. 6.** Representative electron microscopy image (4.000 × magnification) showing a basal keratinocyte with intact cell/cell–cell structures at the basement membrane at the junction to the dermis without changes after 4 × 300 s of plasma exposure (FlatPlaSter 2.0).

The easiest way to study the effects of CAPs on *ex vivo* skin is to make a histological evaluation, which gives the investor information about the tissue tolerability. In our experiments no changes occurred between CAP treated skin and the controls, even after long application times of up to 20 min, which is more than 20 times higher than the actually planned treatment time in subsequent clinical trials. The same result was obtained for both plasma devices. The collective of patients included aged patients—some of them with skin tumors, which are associated with a long-term cumulative dose of sun exposure. Sun damages, such as actinic elastosis can histologically occur in those samples, but as the patient himself acts as his own control, these changes were found in the controls as well.

To get additional safety information and a more detailed look on the cell compartments and structures we realized in a next step electron microscopy (EM) experiments. We concentrated on samples with the longest exposure time of 20 min using the FlatPlaSter 2.0 device. No structural damages were detected in epidermal and dermal cell structures/organelles.

Several groups reported DNA damages after certain dosages of plasma exposure in cells or in different pathogens [31–33]. Most of the analyzed DNA damages were single strand breaks [34], which are easier to repair for human cells [35]. However, double strand breaks can occur as well, depending on the plasma device and the respective setting and dosage [19,33,36]. Kalghatgi et al. [34] used γ-H2AX for the detection of DNA damages in mammalian cells (MCF10A) after plasma treatments (DBD) up to 4.65 J/cm$^2$. The number of DNA damages increased with increasing doses, however they detected no formation of bulky adducts/thymine dimers in their in vitro assay, which may be explained by the formation of single stranded DNA breaks or a replication arrest.

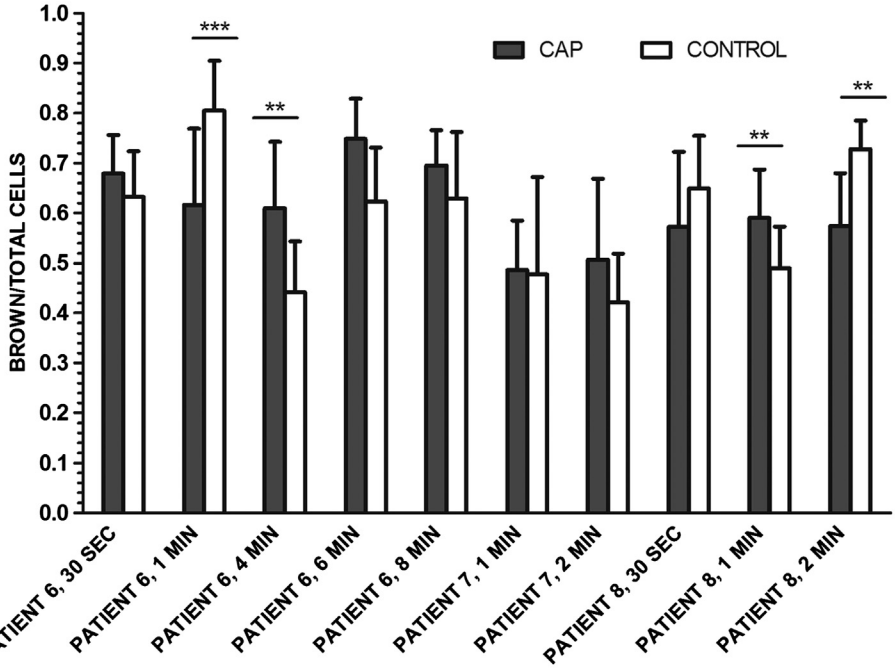


**Fig. 7.** Results of the γ-H2AX staining. The *x*-axis shows the patients number and the respective plasma treatment time. The *y*-axis gives the ratio of stained (brown) cells (i.e. cells possessing DNA double strand breaks)/total number of cells including standard deviation. Significant changes are indicated by ** for *p*-values $\leq 0.05$, highly significant changes by *** for *p*-values $\leq 0.01$. The error bars refer to the standard deviation.

Nevertheless some double strand breaks are irreparable for cells and this is why the investigation of possible DNA damages is obligatory prior to application in human beings.

In this trial we therefore used the γ-H2AX test to detect DNA double strand breaks in *ex vivo* human skin. The results showed, that there were significant higher, but also significant lower changes in detected DNA damages in plasma treated skin samples compared to the controls. This interesting finding that control samples showed sometimes higher DNA damages cannot be explained clearly, since controls were derived from the same patient, from a very close location, from one skin sample and both samples received the same procedure, including the same storage. However, this underlines that our plasma application did not result systematically in higher DNA damages than non-treated skin. Data revealed only a trend to higher damages in plasma treated samples, which were treated for more than 120 s. Plasma treatments up to 60 s could therefore be considered as a safe application time. Interestingly, there was a negative correlation (data not published) between total cell numbers and cell damages. This means that a higher initial cell load could have protective means for other cells from further damage. But damages were not predominantly located in higher layers of cells. Similar findings were shown for plasma applications in biofilms [7]. Subsequent studies will have to investigate the impact of several cell layer depths on DNA damages after plasma application.

Generally, the rate of damages was relatively high (in plasma treated samples and the controls), which can be partly explained by the patients' characteristics, since the patients' age was advanced coming along with a high cumulative dose of UV over the years [37].

In future it is preferable to carry out these experiments in a younger collective of patients to minimize independent changes or UV damages to facilitate the subsequent evaluation process.

Generally it is not clear yet which component of the "plasma cocktail" could contribute to possible DNA damages. It is known that by-products of lipid peroxidation and high concentrations of exogenous reactive species such as hydrogen peroxide, singlet oxygen, hydroxyl radicals, and superoxide radicals can lead to genetic instabilities in cells [37–39]. Since the UV dose is very low for both plasma devices—even for treatment times of up to 8 min the UV dose is below ICNIRP safety limits—we expect that the produced reactive species, especially the reactive oxygen species may play a predominant role [34]. Further studies are needed to clarify the major players.

Measurements and calculations of toxic by-products ($O_3$, NO, and $NO_2$) and the UV power density are in the safe range according to international recommendations/guidelines [28–30]. However, these recommendations/guidelines are not adapted to new treatment approaches like CAP applications and need to be reevaluated.

In conclusion, we believe that experiments using *ex vivo* human skin are inevitable for the investigation of the skin tolerability of emerging CAP devices. Histology and electron microscopy experiments are very easy to realize and give a lot of information on the tissue tolerability. γ-H2AX test did reveal significant higher DNA damages in plasma treated skin samples, but also controls. Longer exposure times ( $>60$ s) trend to have higher DNA damages. The results of the three *ex vivo* experiments obtained in this study demonstrate that plasma treatments up to 60 s using MiniFlatPlaSter and FlatPlaSter 2.0 device are safe and tolerable for the skin.

## Acknowledgements

This study was supported by the Max-Planck Society under Grant no. 02.M.TT.A. We thank I. Höpner for the great help in preparing all samples for the gamma H2AX staining and we are indebted to T.G. Klämpfl for the support and his advices in designing and preparing the devices, same as to W. Bunk, T. Aschenbrenner and R. Monetti for the great help with statistics.

## References

[1] Klampfl TG, Isbary G, Shimizu T, Li YF, Zimmermann JL, Stolz W, et al. Cold atmospheric air plasma sterilization against spores and other microorganisms of clinical interest. Applied and Environmental Microbiology 2012;78:5077–82.
[2] Maisch T, Shimizu T, Isbary G, Heinlin J, Karrer S, Klampfl TG, et al. Contact-free inactivation of *Candida albicans* biofilm by cold-atmospheric air plasma. Applied and Environmental Microbiology 2012;78:4242–7.
[3] Maisch T, Shimizu T, Li Y-F, Heinlin J, Karrer S, Morfill G, et al. Decolonisation of MRSA, *S. aureus* and *E. coli* by cold-atmospheric plasma using a porcine skin model in vitro. PloS One 2012;7:e34610.
[4] Morfill GE, Shimizu T, Steffes B, Schmidt HU. Nosocomial infections—a new approach towards preventive medicine using plasmas. New Journal of Physics 2009;11:1–10.
[5] Niemira BA. Cold plasma reduction of *Salmonella* and *Escherichia coli* O157:H7 on almonds using ambient pressure gases. Journal of Food Science 2012;77:M171–5.
[6] Zimmermann JL, Dumler K, Shimizu T, Morfill GE, Wolf A, Boxhammer V, et al. Effects of cold atmospheric plasmas on adenoviruses in solution. Journal of Physics D: Applied Physics 2011;44:1–9.
[7] Ermolaeva SA, Varfolomeev AF, Chernukha MY, Yurov DS, Vasiliev MM, Kaminskaya AA, et al. Bactericidal effects of non-thermal argon plasma in vitro, in biofilms and in the animal model of infected wounds. Journal of Medical Microbiology 2011;60:75–83.
[8] Ermolaeva SA, Sysolyatina EV, Kolkova NI, Bortsov P, Tuhvatulin AI, Vasiliev MM, et al. Non-thermal argon plasma is bactericidal for the intracellular bacterial pathogen *Chlamydia trachomatis*. Journal of Medical Microbiology 2012;61:793–9.
[9] Lademann J, Richter H, Schanzer S, Patzelt A, Thiede G, Kramer A, et al. Comparison of the antiseptic efficacy of tissue-tolerable plasma and an octenidine hydrochloride-based wound antiseptic on human skin. Skin Pharmacology and Physiology 2012;25:100–6.
[10] Lademann O, Kramer A, Richter H, Patzelt A, Meinke MC, Roewert-Huber J, et al. Antisepsis of the follicular reservoir by treatment with tissue-tolerable plasma (TTP). Laser Physics Letters 2011;8:313–7.
[11] Lademann O, Richter H, Meinke MC, Patzelt A, Kramer A, Hinz P, et al. Drug delivery through the skin barrier enhanced by treatment with tissue-tolerable plasma. Experimental Dermatology 2011;20:488–90.
[12] Shimizu T, Zimmermann JL, Morfill GE. The bactericidal effect of surface micro-discharge plasma under different ambient conditions. New Journal of Physics 2011;13:1–7.
[13] Bender C, Partecke L-I, Kindel E, Doering F, Lademann J, Heidecke C-D, et al. The modified HET-CAM as a model for the assessment of the inflammatory response to tissue tolerable plasma. Toxicology in Vitro 2011;25:530–7.
[14] Kalghatgi S, Fridman G, Fridman A. Non-thermal dielectric barrier discharge plasma treatment of endothelial cells. In: Proceedings of the 30th IEEE engineering in medicine and biology society; 2008. p. 3578–81.
[15] Kalghatgi S, Friedman G, Fridman A, Clyne AM. Endothelial cell proliferation is enhanced by low dose non-thermal plasma through fibroblast growth Factor-2 release. Annals of Biomedical Engineering 2010;38:748–57.
[16] Nosenko T, Shimizu T, Morfill GE. Designing plasmas for chronic wound disinfection. New Journal of Physics 2009;11:1–19.
[17] Pompl R, Jamitzky F, Shimizu T, Steffes B, Bunk W, Schmidt H-U, et al. The effect of low-temperature plasma on bacteria as observed by repeated AFM imaging. New Journal of Physics 2009;11:1–11.
[18] Tipa RS, Kroesen GMW. Plasma-stimulated wound healing. IEEE Transactions on Plasma Science 2011;39:2978–9.
[19] Sensenig R, Kalghatgi S, Cerchar E, Fridman G, Shereshevsky A, Torabi B, et al. Non-thermal plasma induces apoptosis in melanoma cells via production of intracellular reactive oxygen species. Annals of Biomedical Engineering 2011;39:674–87.
[20] Heinlin J, Isbary G, Stolz W, Zeman F, Landthaler M, Morfill G, et al. A randomized two-sided placebo-controlled study on the efficacy and safety of atmospheric non-thermal argon plasma for pruritus. J Eur Acad Dermatol Venereol http://dx.doi.org/10.1111/j.1468-3083.2011.04395.x, in press.
[21] Isbary G, Heinlin J, Shimizu T, Zimmermann JL, Morfill G, Schmidt HU, et al. Successful and safe use of 2 min cold atmospheric argon plasma in chronic wounds: results of a randomized controlled trial. British Journal of Dermatology 2012;167:404–10.
[22] Isbary G, Morfill G, Schmidt HU, Georgi M, Ramrath K, Heinlin J, et al. A first prospective randomized controlled trial to decrease bacterial load using cold atmospheric argon plasma on chronic wounds in patients. British Journal of Dermatology 2010;163:78–82.
[23] Isbary G, Morfill G, Zimmermann J, Shimizu T, Stolz W. Cold atmospheric plasma: a successful treatment of lesions in Hailey-Hailey disease. Archives of Dermatology 2011;147:388–90.

[24] Heinlin J, Isbary G, Stolz W, Morfill G, Landthaler M, Shimizu T, et al. Plasma applications in medicine with a special focus on dermatology. Journal of the European Academy of Dermatology and Venereology 2011;25:1–11.
[25] Heinlin J, Morfill G, Landthaler M, Stolz W, Isbary G, Zimmermann JL, et al. Plasma medicine: possible applications in dermatology. Journal der Deutschen Dermatologischen Gesellschaft 2010;8:968–76.
[26] Kong MG, Kroesen G, Morfill G, Nosenko T, Shimizu T, van Dijk J, et al. Plasma medicine: an introductory review. New Journal of Physics 2009;11:1–35.
[27] Kogelschatz U. Dielectric-barrier discharges: their history, discharge physics, and industrial applications. Plasma Chemistry and Plasma Processing 2003;23: 1–46.
[28] Guidlines on limits of exposure to ultraviolet radiation of wavelengths between 180 nm and 400 nm (incoherent optical radiation): ICNIRP (International Commission on Non-Ionizing Radiation Protection); 2004.
[29] Center for Disease Control and Prevention (CDC) Ozone: NIOSH (National Institute for Occupational Safety and Health).
[30] International Electrotechnical Commission IEC 60601 Medical equipment/ medical electrical equipment—Part 1.
[31] Yasuda H, Miura T, Kurita H, Takashima K, Mizuno A. Biological evaluation of DNA damage in bacteriophages inactivated by atmospheric pressure cold plasma. Plasma Processes and Polymers 2010;7:301–8.
[32] Vandamme M, Robert E, Lerondel S, Sarron V, Ries D, Dozias S, et al. ROS implication in a new antitumor strategy based on non-thermal plasma. International Journal of Cancer 2012;130:2185–94.
[33] O'Connell D, Cox LJ, Hyland WB, McMahon SJ, Reuter S, Graham WG, et al. Cold atmospheric pressure plasma jet interactions with plasmid DNA. Applied Physics Letters 2011;98:1–3.
[34] Kalghatgi S, Kelly CM, Cerchar E, Torabi B, Alekseev O, Fridman A, et al. Effects of non-thermal plasma on mammalian cells. PloS One 2011;6:1–11.
[35] Friedberg EC. How nucleotide excision repair protects against cancer. Nature Reviews Cancer 2001;1:22–33.
[36] Leduc M, Guay D, Coulombe S, Leask RL. Effects of non-thermal plasmas on DNA and mammalian cells. Plasma Processes and Polymers 2010;7:899–909.
[37] Durant ST, Paffett KS, Shrivastav M, Timmins GS, Morgan WF, Nickoloff JA. UV radiation induces delayed hyperrecombination associated with hypermutation in human cells. Molecular and Cellular Biology 2006;26:6047–55.
[38] DeFedericis HC, Patrzyc HB, Rajecki MJ, Budzinski EE, Iijima H, Dawidzik JB, et al. Singlet oxygen-induced DNA damage. Radiation Research 2006;165: 445–51.
[39] Marnett LJ. Lipid peroxidation—DNA damage by malondialdehyde. Mutation Research: Fundamental and Molecular Mechanisms of Mutagenesis 1999;424: 83–95.